Electronic Supplementary Material (ESI) for Nanoscale.

Supporting Information

KPFM visualisation of the Schottky Barrier at the interface between gold nanoparticle and silicon

Luis Lechaptois[*a, b], Yoann Prado[a] and Olivier Pluchery[*a]

[a] Institut des NanoScience de Paris, Sorbonne University, CNRS, UMR7580, 4 place Jussieu, 75005, Paris, France
[b] Slim Lab, Nanyang Technological University, 70 Nanyang Drive, Singapore

1. SEM images of gold nanoparticles

SEM images of 55 nm gold nanoparticles (AuNPs) deposited on sample A were recorded. AuNPs are immobilized with a monolayer of APTES.

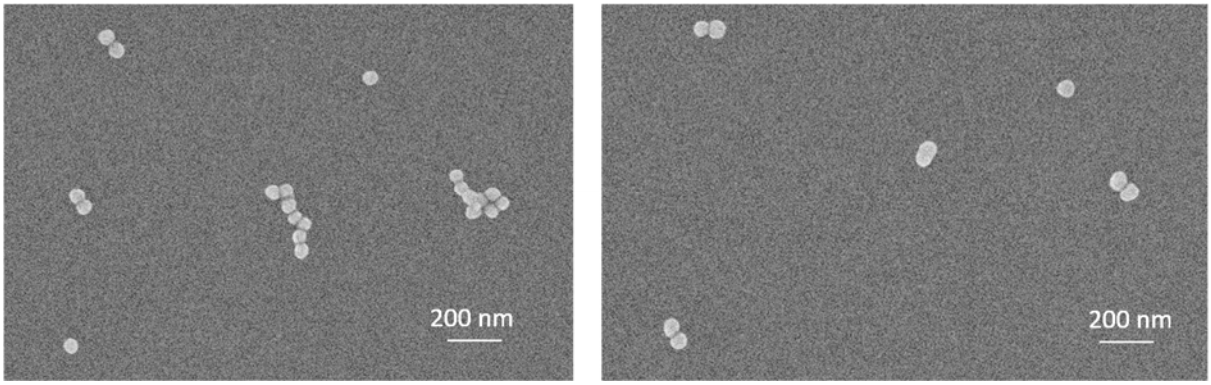

*Figure **S1** : SEM images (2 x 1.5 µm²) of gold nanoparticles on n-doped silicon.*

2. KPFM measurement: influence of the scan rate

Figures S2 below show the KPFM images obtained on sample A with three different scan rates. All the CPD images exhibit the ring-shaped patterns at every scan rate. This confirms that this pattern in the potential images is not an artefact from this parameter. However, at a high scan rate (3000 nm/s), the ring tends to become dissymmetric. This is why all the other images were recorded with a scan rate of 750 nm/s.

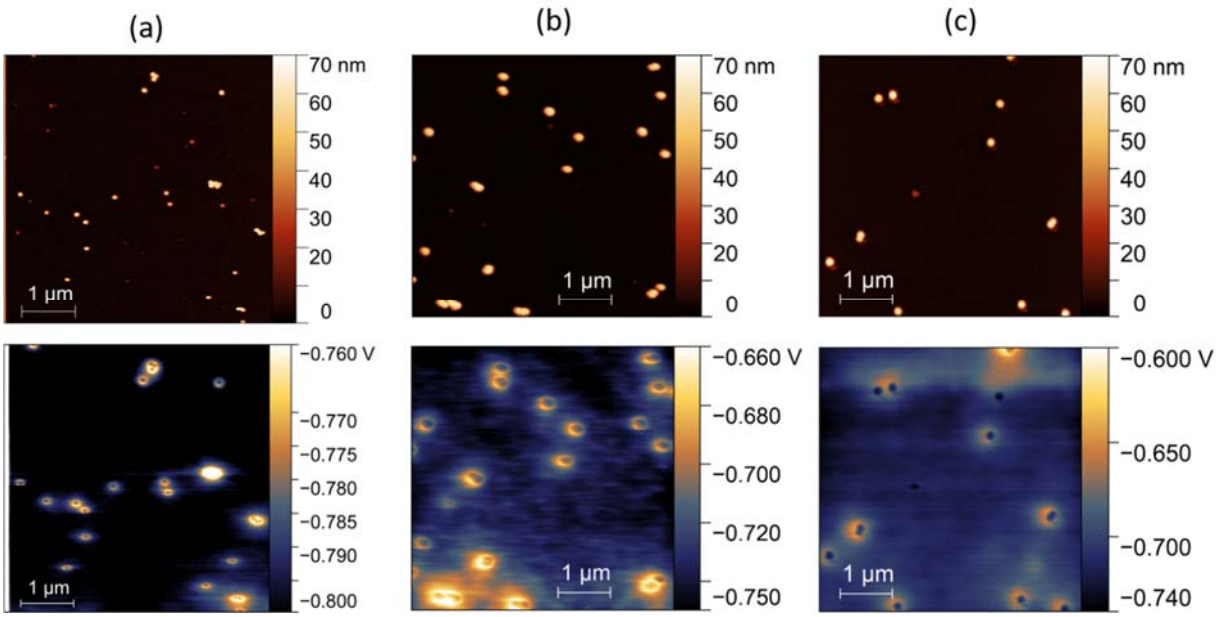

*Figure **S2** : Topography (top) and relative CPD (bottom) images (5 x 5 µm²) of gold nanoparticles on n-doped silicon obtained at different scan rates: (a) 750 nm.s^{-1}; (b) 2250 nm.s^{-1}; (c) 3000 nm.s^{-1}.*

3. KPFM measurement: influence of the Lift Scan Height (LSH)

The figures S3 below show KPFM images of the same area obtained on sample A at 5 different LSH. The table S1 summarizes the values of the built-in potential Φ_{bi} when the LSH is decreased. For LSH < 40 nm, CPD images exhibits a convolution artefact on the gold nanoparticles due to unpredictable contact between the tip and the sample. The values for Φ_{bi} become unreliable. At LSH = 20 nm, the ring-shaped pattern is no longer visible.

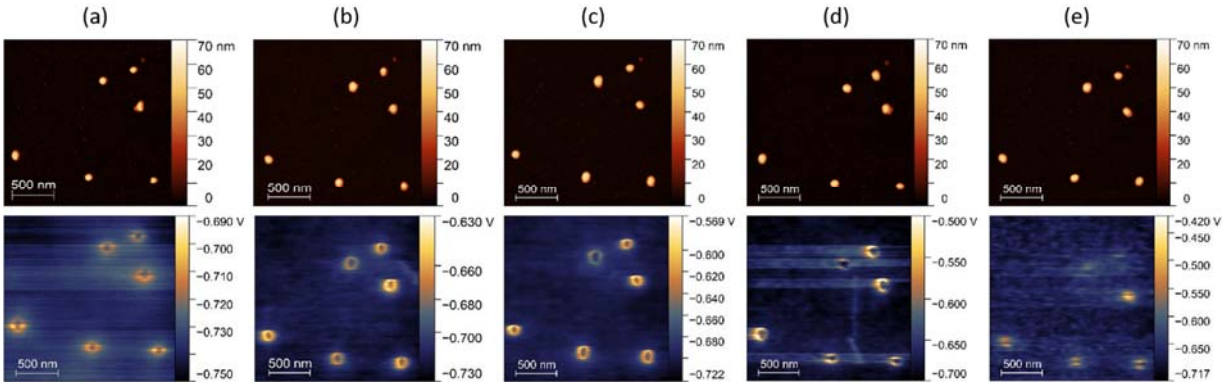

*Figure **S3** : Topography (top) and relative CPD (bottom) images of 55 nm AuNPs on n-doped silicon obtained at different LSH: (a) 70 nm; (b) 50 nm (c) 40 nm; (d) 30 nm; (e) 20 nm.*

LSH (nm)	70	60	50	40	30	20
Φ_{bi} (mV)	30	34	65	80	30-120 (*)	0-100 (*).

Table S1. Values of the built-in potential for decreasing values of the LSH from 70 to 20 nm. Values marked with (*) indicate unreliable data caused by a too low value of the LSH.

4. KPFM measurement: checking the uniformity of the APTES monolayer

These images in Fig. S4 below emphasize the small irregularities of the APTES monolayer. The topographic image in Fig. S4a shows small grains originated be APTES aggregates of typically 1 nm. The corresponding CPD variations are around 1 mV. These small variations do not screen the CPD variations induced by the AuNPs which are in the order of magnitude of 30 mV.

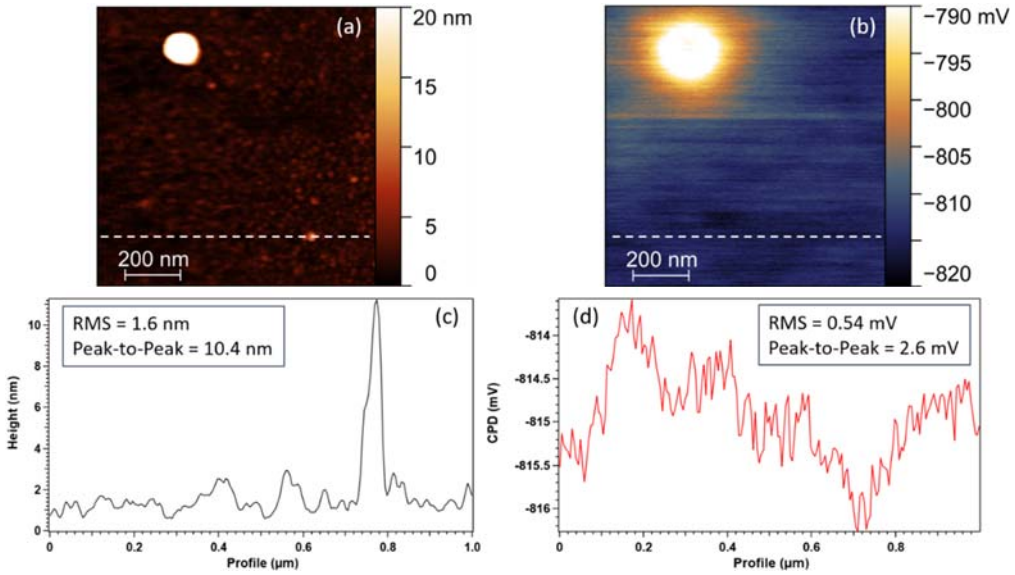

*Figure **S4** : Topography image (a) and its corresponding CPD image (b) of one gold nanoparticle on n-doped silicon (sample A). Profiles (from white dashed line) below show the height (c) and CPD (d) of a part of the APTES monolayer. Root Mean Square (RMS) and Peak-to-Peak values along these lines are displayed in insert of the graphs.*

5. KPFM images of AuNPs on p-doped silicon

The CPD image below show gold nanoparticles on *p*-doped silicon. They also exhibit a ring-shaped pattern, but of much smaller amplitude.

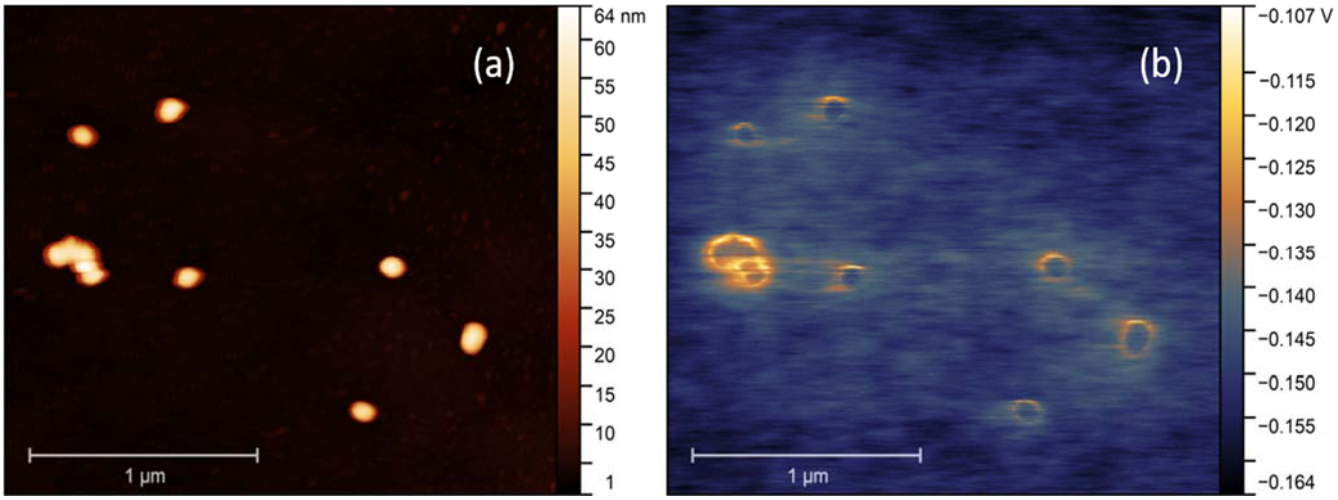

*Figure **S5**: KPFM topography (a) and CPD (b) images of gold nanoparticles on p-doped silicon wafer (N_D = 10^{14}-$10^{15}cm^{-3}$).*

6. Distributions of barrier heights

From the KPFM images, the potential barriers were measured for 32 different AuNPs. The values are represented with the histograms given in Fig. S6. It shows an average potential rise of 34.3 ± 0.6 mV for the *n*-doped and 21.2 ± 1.0 mV for *p*-doped. This potential rise corresponds to the built-in potential Φ_{bi}.

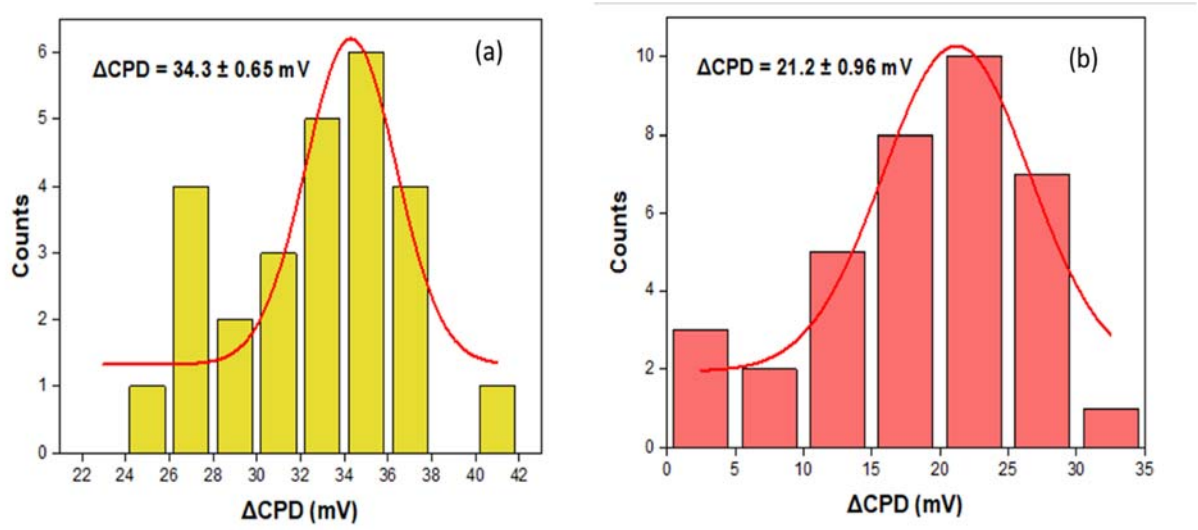

*Figure **S6**: Distributions of ΔCPD measured for gold nanoparticles on n-doped (a) and p-doped (b) silicon substrates. In both cases the dopant concentration was 10^{15} cm^{-3} (10-20 Ω.cm).*

7. Band bending calculation from *Band Diagram Program*

Fig. S7 is a representation of the results obtained with the *Band Diagram Program* developed by Knowlton in the two cases of Fig 5 in the main text. The top band diagram of Fig. S7 corresponds to a planar ideal interface gold/SiO_2/Si. It results in a built-in potential of 660 mV. The second band diagram correspond to system that includes a gap of 10 nm of air and mimics a situation of the silicon surface in the vicinity of the AuNPs and not exactly below it. This crude description demonstrates that the built-in potential reduces to 520 mV. As explained in the main text, this explains the progressive CPD increase when the KPFM tip approaches a AuNP.

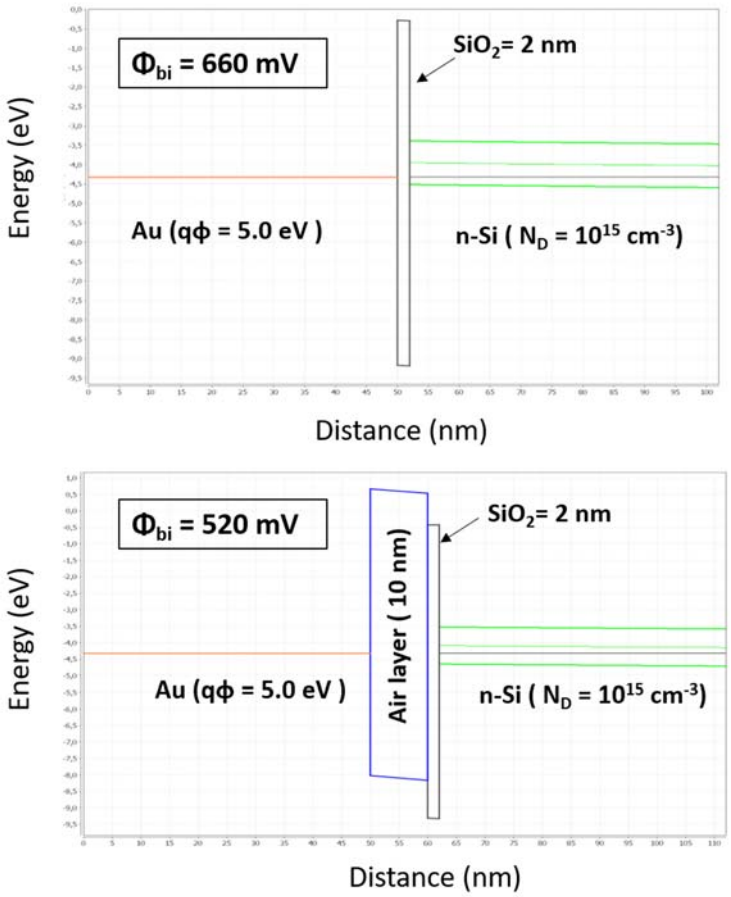

*Figure **S7**: Band Bending simulation with an air layer of 320 nm (up) and 10 nm (down). Respective Φ_{bi} are 660 mV and 520 mV.*